The benefits of hybridising electrodialysis with reverse osmosis

Ronan K. McGovern[a], Syed M. Zubair[b], John H. Lienhard V[a]

[a] *Center for Clean Water and Clean Energy, Massachusetts Institute of Technology, Cambridge, MA 02139, United States*
[b] *King Fahd University for Petroleum and Minerals, Dhahran, Saudi Arabia*

Abstract

A cost analysis reveals that hybridisation of electrodialysis with reverse osmosis is only justified if the cost of water from the reverse osmosis unit is less than 40% of that from a stand–alone electrodialysis system. In such cases the additional reverse osmosis costs justify the electrodialysis cost savings brought about by shifting salt removal to higher salinity, where current densities are higher and equipment costs lower. Furthermore, the analysis suggests that a simple hybrid configuration is more cost effective than a recirculated hybrid, a simple hybrid being one where the reverse osmosis concentrate is fed to the electrodialysis stack and the products from both units are blended, and a recirculated being one hybrid involving recirculation of the electrodialysis product back to the reverse osmosis unit. The underlying rationale is that simple hybridisation shifts salt removal away from the lowest salinity zone of operation, where salt removal is most expensive. Further shifts in the salinity at which salt is removed, brought about by recirculation, do not justify the associated increased costs of reverse osmosis.

Keywords: reverse osmosis, electrodialysis, hybrid

1. Introduction

Based on a comparison of the cost of water, we establish guidelines for choosing between stand–alone electrodialysis (ED) and hybrid electrodialysis-reverse osmosis (ED–RO) systems. By modelling the energy and equipment costs of electrodialysis as a function of product salinity we demonstrate the opportunity to reduce costs by shifting salt removal to higher salinity. Hybridisation of electrodialysis with reverse osmosis allows such a shift. Therefore, we model hybrid electrodialysis-reverse osmosis systems to establish when the benefits of hybridisation outweigh the costs of the reverse osmosis unit. We frame our models such that the decision between hybrid and stand–alone systems is based upon a cost ratio between reverse osmosis and electrodialysis systems, and consider this as a variable in our analysis.

Our interest in hybrid ED–RO systems is to further minimise the environmental impact and economic cost of brackish desalination, of which the latter has grown at an estimated annualised rate of 12% over the past 10 years [1] (see Appendix A). Brackish desalination involves the treatment of waters of slight (1,000-3,000 ppm total dissolved solids, TDS) to moderate salinity (3,000-10,000 ppm TDS) [2] present in naturally saline inland aquifers or coastal aquifers that have become subject to the intrusion of seawater [3] (see Fig. 1).

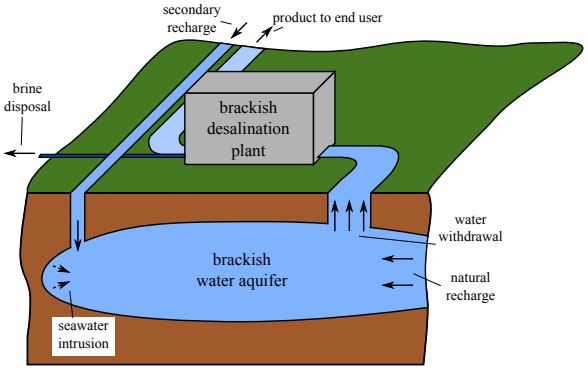

Figure 1: The supply of freshwater and mitigation of seawater intrusion with brackish desalination and secondary recharge. Based on an aquifer management system proposed by Koussis et al. [4].

Email addresses: mcgov@alum.mit.edu (Ronan K. McGovern), lienhard@mit.edu (John H. Lienhard V)

From environmental and cost perspectives, the ratio of water recovered to that withdrawn, known as the recovery ratio, *RR*, is an important consideration. A higher recovery ratio allows the following benefits: a reduction in the size of the desalination plant intake; a reduction in the volume of brine produced, which requires disposal to the sea, surface waters or confined aquifers below the aquifer from which water is withdrawn [5]; and a reduction in the rate of aquifer recharge required, which might be done continuously with treated waste water [4] or periodically with water sourced from another location during periods of low demand [6]. Conversely, a higher recovery ratio results in the production of higher salinity brine, which, depending upon the degree of dispersion and/or dilution employed at the point of disposal, can have adverse effects on plant and animal life [7]. We focus on scenarios where the benefits of reduced volumes outweigh those of increased salinity and consider technologies offering high recovery ratios.

Electrodialysis is well suited to applications requiring high recovery ratios for at least three reasons. Firstly, electrodialysis is a salt removal rather than a water removal technology, and so the majority of the feed water is easily recovered as a product. This is in contrast to reverse osmosis, where high recovery ratios require multiple stages in a continuous process (Fig. 2a) or longer process times in a semi-batch (or batch) process [8]. Secondly, electrodialysis is capable of reaching brine concentrations above 10% total dissolved solids (TDS), which is beyond the osmotic pressures reachable by current reverse osmosis systems [9, 10]. Thirdly, seeded precipitation of scalants in the ED process can in some cases circumvent the barrier on water recovery imposed by the solubility of feedwater solutes; this has been demonstrated by recirculating the electrodialysis concentrate loop through a crystalliser [9, 11, 12] or a combination of a crystalliser and an ultrafiltration unit [10].

Although ED enjoys the advantage of high water recovery, costs increase with the amount of salt removal required (Fig. 2b). This is particularly true at low salinity where salt removal rates, which scale with the electrical current, are limited by the rate of diffusion of ions to the membrane surface. This phenomenon, known as the limiting current density, as well as the high electrical resistance of solutions at low concentrations, increase the costs of electrodialysis at low salinity. Thus, it is the synergy of ED providing high recovery and RO providing final high product purity that gave rise to analyses of hybrid ED–RO systems. The technical feasibility of these systems has already been demonstrated [10, 12–16], but there are a limited number of studies benchmarking hybrid ED–RO systems against other technologies. To date, one study has compared hybrid ED–RO to a reverse-osmosis-mechanical-vapour-compression system and concluded that the hybrid system has lower upfront capital costs and lower operational costs [13].

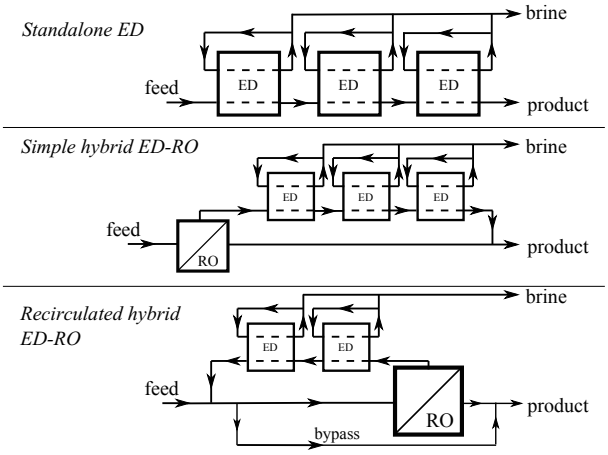

Figure 3: stand–alone and hybrid ED configurations. The relative size of electrodialysis (ED) and reverse osmosis (RO) units is intended to illustrate the relative quantities of membrane area required in each, assuming the final product flow rate from all systems is the same.

In summary, electrodialysis can offer the benefit of higher recovery relative to reverse osmosis systems. Although the cost of water from a reverse osmosis system operating at lower recovery may be smaller, when brine disposal costs are taken into account, electrodialysis can be more cost effective [**?**]. In this paper we focus on scenarios where, overall, ED is more cost effective than RO and analyse the question of when it is preferable to hybridise electrodialysis with reverse osmosis rather than operate with electrodialysis alone. We also compare simple hybrid and recirculated hybrid system configurations.

2. The rationale for hybridising electrodialysis with reverse osmosis

The rationale for hybridising electrodialysis with reverse osmosis is to relax the product purity requirements on the electrodialysis unit. Later, we will demonstrate how these requirements can be relaxed by comparing simple hybrid and recirculated hybrid designs to a stand–alone ED system, Fig. 3. First, to understand why the relaxation of product purity requirements can reduce ED costs, we focus on the stand–alone ED system and consider the dependence of the specific cost of water on product purity.

We consider a steady-state 1-dimensional model for the performance and cost of a stand–alone electrodialysis system. The total system area is divided, in the direction of the flow, into 20 stacks within which salt and water transport are approximated as uniform. These stacks serve the numerical purpose of discretisation and do not relate to the number of stacks within a real

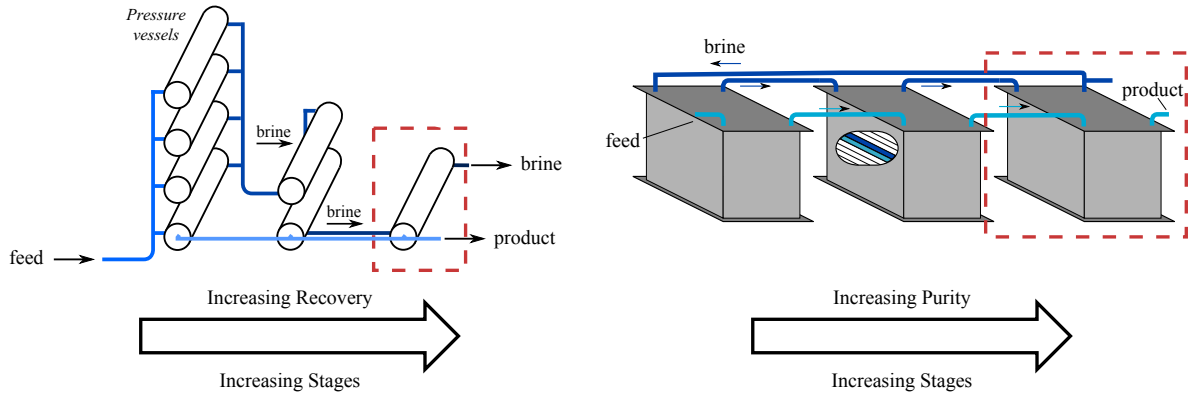

(a) Reverse osmosis

(b) Electrodialysis

Figure 2: The ability of electrodialysis to achieve high recovery and reverse osmosis to achieve high purity points towards an opportunity for hybridisation.

system. The key salt, water and charge transport equations, which are based on the approach of Fidaleo and Moresi [17], and McGovern et al. [18] are then applied to each stack. Membrane properties, flow rates and cell pair parameters are also taken from Fidaleo and Moresi [17] and are provided in Appendix B. The process is designed and costed according to the following specifications and assumptions:

1. the feed is aqueous NaCl;
2. the concentrate concentration within each stack is determined by the net rates of salt and water transport across the membranes;
3. the system is operated at voltage of 0.8 V which corresponds to just above 70% of the limiting current density [19] (see Appendix B.2);
4. equipment and stack energy costs are considered but pumping power is neglected (see Appendix G);
5. equipment is costed on the basis of membrane area at \$1500/m^2 of cell pair area (see Appendix C), amortised at 10% over 20 years;
6. energy costs are computed on the basis of stack power consumption (see Appendix D for validation of results) and a 0.065 \$/kWh cost of electricity; and
7. the product flow rate is set at 1,000 m^3/day.

Specifying the feed salinity along with the product salinity and flow rate, these equations are solved simultaneously using a non-linear equation solver [20] to compute the final concentrate concentration, total membrane area, energy consumption, specific equipment costs, specific energy costs, and specific water costs.

Figure 4a illustrates the dependence of the specific cost of water C upon the product salinity S_P while Fig 4b illustrates the dependence of the marginal cost

$$MC = \frac{\partial C}{\partial S_d}, \tag{1}$$

upon the local diluate salinity S_d, the low salinity stream within an ED process (as opposed to the high salinity recirculated concentrate stream). These figures show that the marginal cost of salt removal decreases with increasing diluate salinity. The marginal cost of equipment falls since the current density increases with salinity and more salt is removed per unit of membrane area. The marginal cost of energy per unit of salt removed equals the power density (current density times cell pair voltage iV^{cp}) divided by the rate of salt removal (which scales with the current density i). Therefore the marginal cost of energy is approximately proportional to the cell pair voltage V^{cp} and relatively constant. Fig 4b illustrates an important opportunity to reduce ED costs by shifting salt removal to higher salinity.

Figure 5 illustrates the impact of shifting salt removal to higher salinity. In a stand–alone ED system salt is removed over a range from 3,000 ppm (the feed salinity) to 350 ppm (the product salinity). If, via hybridisation, salt could be removed at 3,000 ppm the specific cost of water would be represented by the rectangular area in Fig. 5 rather than the total area under the marginal cost curve. Figure 5 also shows that savings diminish as salt removal shifts to higher and higher salinity. This allows us to conclude that the percentage cost reduction in ED achieved through hybridisation:

1. is greatest when salt removal occurs at low salinity, *e.g.* when feed and product salinity are low
2. is smallest when salt removal occurs at high salinity, *e.g.* when feed salinity is high and especially

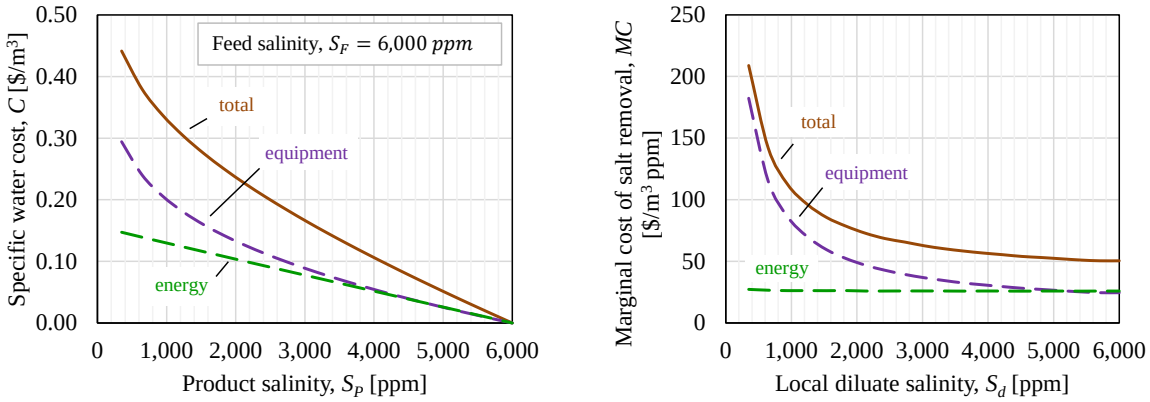

(a) Specific water cost

(b) Marginal cost of salt removal

Figure 4: The falling marginal cost of salt removal with increasing local diluate salinity points to an opportunity to shift salt removal to higher salinities via hybridisation.

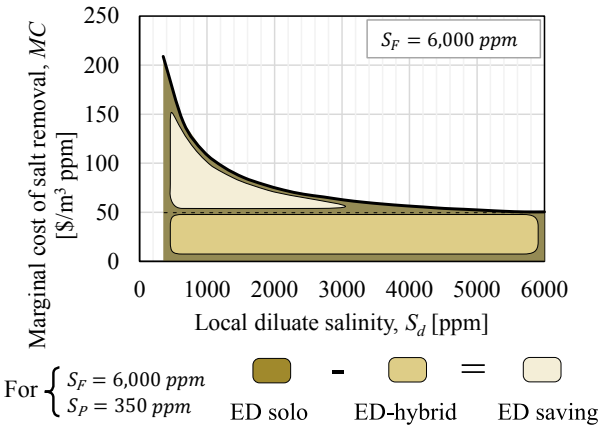

Figure 5: Cost savings can be achieved by shifting electrodialysis salt removal to higher salinity.

when both feed and product salinity are high.

3. Reasons to prefer a simple ED–RO hybrid configuration

One way to shift salt removal to higher salinity is via the simple hybrid ED–RO configuration [12] illustrated in Fig. 3. This configuration has two benefits over a stand–alone electrodialysis system: the total membrane area (or number of stacks required) is reduced as higher rates of salt removal (current densities) are possible at higher salinities; and electrodialysis product requirements are relaxed since the final product consists of a blend of high purity RO permeate and the electrodialysis product. In practise, the recovery ratio of the reverse osmosis unit in the simple hybrid configuration would be a design variable. Increasing the recovery ratio leads to increasing reverse osmosis costs due to:

1. increased risks of scaling due to higher brine concentrations;
2. higher energy costs due to an increasing osmotic pressure;
3. the need for a second stage of reverse osmosis if recoveries above 50% are required [8].

Increasing recovery ratios would also lead to reduced salt removal costs in the ED unit as the cost of salt removal falls at higher diluate salinities (see Fig. 5). This means that the recovery ratio would be set by a trade-off between reverse osmosis and electrodialysis costs. Furthermore, since, according to Fig. 5, there are diminishing returns as the ED feed salinity is increased the optimal recovery ratio is likely to be low if the system feed salinity is high and high if the system feed salinity is low. We leave the optimisation of the reverse osmosis recovery ratio to future work and, in this analysis, focus upon hybrid designs involving a single stage reverse osmosis unit treating feed streams of 3,000 ppm TDS and operating at 50% recovery. This puts the feed salinity to the ED unit at 6,000 ppm TDS, a point at which the change in salt removal costs with diluate salinity is already weak (Fig. 5).

To guide a decision between a stand–alone ED system and a simple ED–RO hybrid we require a measure of the relative cost of water from reverse osmosis and electrodialysis. In practise, one can envision costing a single-stage reverse osmosis unit operating at 50% recovery for a given feedwater flow rate and salinity. One can also envision costing (as we have done) water from a stand–alone electrodialysis system operating at a desired recovery ratio. Hence, in defining the cost ratio CR, we consider the the cost of water from a single-stage RO unit to that from a stand–alone ED

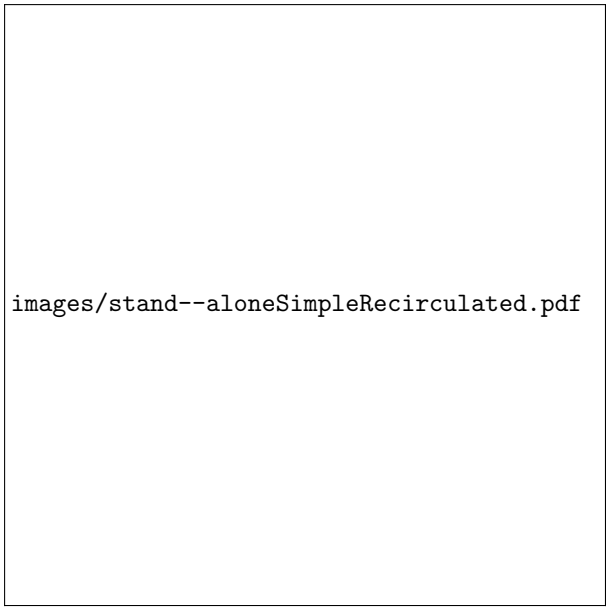

Figure 6: Dependence of the optimality of hybrid systems upon the cost ratio and the product salinity.

unit. Specifically, the cost ratio is defined as the cost of water from an RO unit operating at 50% recovery $C_{RO}^{50\%}$ divided by the cost of water from an ED unit treating the same feedwater down to a desired product salinity, C_{ED}:

$$CR \equiv \frac{C_{RO}^{50\%}}{C_{ED}} \tag{2}$$

Applying equations describing the continuity of mass at the point of blending and across the reverse osmosis unit in Fig 5, and making the assumptions of:

- feed water at 3,000 ppm TDS,
- a recovery ratio of 50% in the reverse osmosis unit, and
- a reverse osmosis product salinity of 50 ppm

we can compute value of CR at which the cost of water from a stand–alone ED and simple ED–RO hybrid systems are the same, which we define as the critical cost ratio CR^*. Detailed calculations are shown in Appendix E. Importantly, the overall recovery of feed water as product water from both the simple hybrid and the stand–alone ED systems are almost the same. This is because similar amounts of water cross from the diluate to the concentrate stream via osmosis or electro-osmosis in the ED unit of both systems (see Appendix F). Differences in volumes of waste brines produced by both systems are therefore ignored.

Figure **??** shows that when high product purity is required (S_P = 50 ppm TDS) a simple hybrid ED–RO configuration is preferred if the cost of water from a single-stage RO unit is less than 70% of the cost of water from a stand–alone ED system. If potable water purity (500 ppm TDS) is required the relative cost of water from a single-stage RO system would have to be 65% of that from stand–alone ED to justify hybridisation. If product water requirements are even more relaxed (1,000 ppm TDS) the cost savings are smaller and it is even less likely for a hybrid to be preferred.

The dependence of the critical cost ratio CR^* upon product salinity, for the simple-hybrid, may be explained through consideration of the following equation equating the cost of a stand–alone and a simple hybrid system:

$$C_{ED}^{solo}\dot{V}_P = C_{ED}^{hybrid}\dot{V}_{ED,P} + C_{RO}^{hybrid}\dot{V}_{RO,P}, \tag{3}$$

or, given a reverse osmosis recovery ratio of 50%:

$$C_{ED}^{solo} \approx \frac{1}{2}\left(C_{ED}^{hybrid} + C_{RO}^{hybrid}\right) \tag{4}$$

where C_{ED}^{solo}, C_{ED}^{hybrid} and C_{RO}^{hybrid} are the specific costs of water from electrodialysis units operating in stand–alone and hybrid configurations, and from the reverse osmosis unit in the hybrid configuration. $\dot{V}_P$, $\dot{V}_{ED,P}$ and $\dot{V}_{RO,P}$ are the volume flow rates of water from entire stand–alone or hybrid systems, from the ED unit within the hybrid and from the RO unit within the hybrid, respectively. Rearranging the above equation and introducing the critical cost ratio $CR^* \equiv C_{RO}^{hybrid}/C_{ED}^{solo}$, we see that the critical price ratio increases when the ratio of water costs from ED in the hybrid to the stand–alone system decreases:

$$CR^*\dot{V}_{RO,P} = \dot{V}_P - \frac{C_{ED}^{hybrid}}{C_{ED}^{solo}}\dot{V}_{ED,P} \tag{5}$$

$$CR^* \approx 2 - \frac{C_{ED}^{hybrid}}{C_{ED}^{solo}}. \tag{6}$$

Comparing ED units operating in stand-alone and simple-hybrid configurations, the ED unit within a stand-alone configuration will always have to desalinate the feed down to higher purity. Thus, considering Fig. 4b, the marginal cost of reducing ED product salinity will always be higher for the stand–alone system. This effect tends to decrease the cost ratio of ED in a simple-hybrid to a stand–alone ED unit, and thus increase the critical cost ratio CR^*. However, at low system product salinities an opposing effect becomes important. Due to the 50% recovery ratio of the RO unit, a marginal decrease in the system product salinity results in approximately double that decrease in the ED product salinity in the hybrid configuration, since:

$$0.5(S_{RO,P} + S_{ED,P}) \approx S_P. \tag{7}$$

Therefore, at low system product salinity, where ED product salinities S_{ED}^{solo} and S_{ED}^{hybrid} are close, and thus

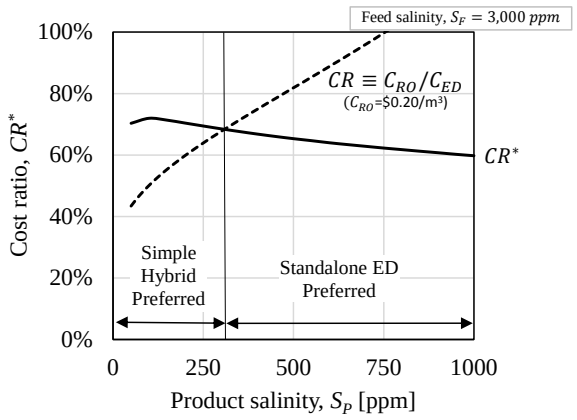

Figure 7: The ratio of water costs from single stage RO rise relative to ED as product salinity increases. At low product salinities a hybrid system can therefore be justified as the cost ratio falls below the critical cost ratio CR^* while at higher product salinities a stand–alone ED system is preferable.

their marginal costs of salt removal (in Fig. 4b) are close, the ratio of $C_{ED}^{hybrid}/C_{ED}^{solo}$ begins to rise and hence CR^* begins to fall.

While the critical price ratio by and large increases as system product salinity falls, there is a further reason why a simple hybrid system is likely to be preferred for high product purity. As product purity increases, ED costs will increase (according to Fig. 4a) and, as a consequence, increase relative to the cost of a single-stage RO system, resulting in a greater chance that CR will fall below CR^*. This is shown in Fig. 7 where the cost ratio is shown for a case where reverse osmosis water costs are \$0.20/m^3 (a reasonable value for brackish reverse osmosis [**?**]). In this scenario a simple hybrid would be preferred if product water salinity below approximately 300 ppm is required while a stand–alone ED system would be preferred for higher product salinities.

4. Reasons to prefer a recirculated hybrid ED–RO system

While the simple hybrid configuration of Fig. 3 can shift salt removal to higher salinities, the hybrid configuration [10, 13–16] that incorporates recirculation can furthermore facilitate salt removal within a narrower band of higher salinity (closer to what is illustrated in Fig. 5). The effect of hybridising with recirculation is thus to cut down more drastically on ED costs than in the simple hybrid configuration, but at the expense of greater reverse osmosis costs, since a majority of product now comes from the reverse osmosis unit. As done for the simple hybrid system, by applying equations describing the continuity of mass at the point of blending and across the reverse osmosis unit in Fig. **??**, and making the assumptions of

- feed water at 3,000 ppm TDS,
- a recovery ratio of 50% in the reverse osmosis unit(s), and
- a reverse osmosis product salinity of 50 ppm,

we can illustrate in Fig. **??** the value of CR^* at which the cost of water from stand–alone ED and recirculated ED–RO hybrid systems are the same.

As with the simple hybrid system, the recirculated hybrid system is more strongly preferred over a stand–alone ED system when high product purities are required. However, regardless of product purity requirements, the recirculated system is inferior to the simple hybrid system, as indicated by a lower value of CR^*. In other words, if moving from a simple to a recirculated hybrid, the additional reverse osmosis costs do not justify the additional ED savings brought about by further shifting salt removal to higher salinity. One way to explain this is that, returning to Fig. 5, the greatest savings are made by shifting salt removal away from the lowest salinities and a simple ED–RO hybrid achieves just this. The reduced savings, achieved by further increasing the concentration at which salt is removed, do not justify the additional reverse osmosis investment involved in a recirculated hybrid.

4.1. Implications of scaling and fouling on the selection of stand–alone versus hybrid systems

In addition to the preceding analysis, an assessment of the risks of membrane fouling and scaling are essential in guiding choice between stand–alone and hybrid systems.

In moving from a stand–alone ED system to a hybrid with reverse osmosis, pre-treatment will have to be adjusted to meet the requirements of reverse osmosis; the more sensitive of the two. Reverse osmosis feed requirements typically limit the Silt Density Index (SDI) to a maximum of 5 and the free chlorine content to a maximum of 0.1 ppm in the feed water [**?**]. Electrodialysis, by comparison, can tolerate an SDI of 10 and a free chlorine content of 0.5 ppm, as well as fluctuations up to an SDI of 15 and free chlorine of 30 ppm [22].

In the simple hybrid configuration, the concentration of non-ionic and weakly-ionised species will be almost unchanged between the feed to the system and the final product; since weakly-ionised compounds are poorly removed by electrodialysis. The suitability of the simple hybrid will then depend upon whether such species can be tolerated in the product or cost effectively removed after the process. In moving from a simple ED–RO hybrid to a recirculated configuration, weakly-ionised species in the feed would build up within the recirculation loop where their primary means of escape is via the RO bypass, Fig. 5. If such species are low in

solubility (*e.g.* silica [10]) they can potentially precipitate within the electrodialysis or reverse osmosis units. In some cases, species may be encouraged to dissociate into ionic form by pH adjustment [23] which would then allow their removal via electrodialysis. The costs associated with this pH adjustment would have a bearing on the decision of whether to hybridise or not.

Since considerations of scaling and fouling tend to act in favour of stand–alone electrodialysis systems, the effective cost ratio that single-stage RO systems must reach to make hybridisation viable, in particular with recirculation, is likely to be lower than those suggested by the present analysis.

5. Sensitivity analysis

Table 1 provides the sensitivity of the critical cost ratio, CR^*, to key input parameters for a simple hybrid system operating with a feed of 3,000 ppm, a product stream of 500 ppm and an applied voltage per cell pair corresponding to 70% of the limiting current density at 350 ppm. The sensitivity to each input parameter, X, is calculated according to:

$$\Sigma = \frac{X}{CR^*}\frac{\partial CR}{\partial X}. \tag{8}$$

CR^* is more sensitive to percentage changes in the feed salinity S_F than to percentage changes in the product salinity S_P. This is because, for the conditions at which these sensitivities are evaluated, the feed salinity is almost one order of magnitude greater than the product salinity. A 1% change in feed salinity will therefore affect the total salt removal required almost ten times as much as a 1% change in product salinity.

The sensitivity of CR^* to the cell pair area normalised cost of equipment, K_Q, and the specific cost of energy, K_E, may be understood via Fig. 4a. Since capital costs dominate energy costs at low product salinity, CR^* is more sensitive to K_Q than K_E.

Finally, to understand the sensitivity of CR^* to cell pair voltage, V_{cp}, we can consider the effect of cell pair voltage upon the marginal cost of salt removal. Three voltages are considered in Fig. 8 that correspond to 50%, 70% and 90% of the limiting current density at a point in the system where the diluate salinity is 350 ppm (see Appendix B.2). The effect of increasing the cell pair voltage is to increase energy costs but to decrease capital costs, because the current drawn is higher. This results in a flattening of the marginal cost curve as the energy cost component becomes more significant (see Fig. 4b). Due to the opposing effects of rising energy costs and falling equipment costs with voltage only a small change in the marginal cost curves is seen in Fig. 8, meaning that, over this range of voltages and for the chosen cost parameters, CR^* is weakly affected.

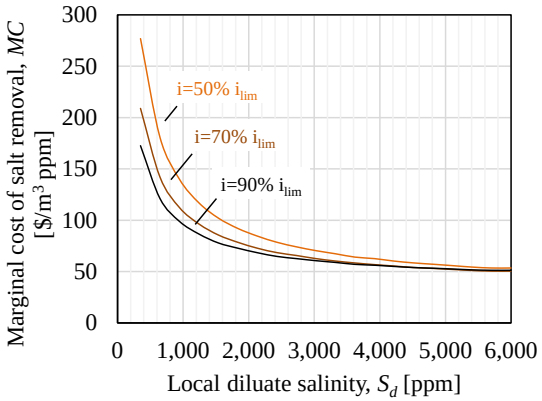

Figure 8: Illustration of the sensitivity of the marginal cost of salt removal to cell pair voltage.

Figure 8 also helps explain the effect of changing specific equipment and electricity prices on CR^*. For the chosen set of cost parameters, Fig. 8 suggests that the optimal strategy is close to 90% of limiting current density. Were specific equipment costs (in \$/m^2 of cell pair area) to decrease relative to the cost of electricity (in \$/kWh) then the marginal cost curve would tend to flatten, thus weakening the benefit of shifting salt removal to higher salinity. However, this flattening would, to some extent, be mitigated since the optimal voltage would be driven down, serving to increase equipment relative to energy costs.

Table 1: Sensitivity of the critical cost ratio

Perturbed Variable	Sensitivity Σ
S_F	0.65
K_Q	0.42
V_{cp}	0.19
K_E	0.14
S_P	0.10

6. Conclusion

Hybrid ED–RO systems will be preferred over stand–alone ED systems where a high purity product is required *and* provided the cost of water from RO is low relative to ED. The break-even point between a hybrid ED–RO and a stand–alone ED system occurs when the cost of water from a single stage RO system, operating at 50% recovery, is between about 60-70% of the cost of water from a stand–alone ED system. At break-even, the savings in ED costs, brought about by the elimination of low salinity stages in a hybrid, justify the added costs of RO. The lower the product salinity required, the greater the potential reduction in ED costs through hybridisation, and hence the higher the

break-even cost ratio (cost of water from single stage RO relative to stand–alone ED).

7. Acknowledgement

The authors are grateful for the support of the Hugh Hampton Young Memorial Fellowship and of the King Fahd University of Petroleum and Minerals through the Center for Clean Water and Clean Energy at MIT and KFUPM under project number R15-CW-11.

References

[1] Desaldata, Analysis, desaldata.com (2013).
[2] S. C. McCutcheon, J. L. Martin, T. Barnwell Jr, D. Maidment, Water quality, 1992. pp.11.1-11.73. In D.R. Maidment (ed.) Handbook of Hydrology. McGraw-Hill, New York, NY.
[3] M. Radmor, J. Strauss, J. Bishop, G. Piatt, K. DeGroat, D. Fargo, D. Eisemann, C. Mulligan, Desalination and water purification technology roadmap, Tech. rep., DTIC Document (2003).
[4] A. Koussis, E. Georgopoulou, A. Kotronarou, D. Lalas, P. Restrepo, G. Destouni, C. Prieto, J. Rodriguez, J. Rodriguez-Mirasol, T. Cordero, A. Gomez-Gotor, Cost-efficient management of coastal aquifers via recharge with treated wastewater and desalination of brackish groundwater: general framework, Hydrological Sciences Journal–Journal des Sciences Hydrologiques 55 (7) (2010) 1217–1233.
[5] N. Wolthek, K. Raat, J. A. de Ruijter, A. Kemperman, A. Oosterhof, Desalination of brackish groundwater and concentrate disposal by deep well injection, Desalination and Water Treatment 51 (4-6) (2013) 1131–1136.
[6] D. A. Blair, W. D. Spronz, K. W. Ryan, Brackish groundwater desalination: A community's solution to water supply and aquifer protection, JAWRA Journal of the American Water Resources Association 35 (5) (1999) 1201–1212.
[7] D. A. Roberts, E. L. Johnston, N. A. Knott, Impacts of desalination plant discharges on the marine environment: A critical review of published studies, water research 44 (18) (2010) 5117–5128.
[8] R. L. Stover, Industrial and brackish water treatment with closed circuit reverse osmosis, Desalination and Water Treatment 51 (4-6) (2013) 1124–1130.
[9] R. Rautenbach, W. Kopp, C. Herion, Electrodialysis-contact sludge reactor and reverse osmosis-phase separator, two examples of a simple process combination for increasing the water recovery rate of membrane processes, Desalination 72 (3) (1989) 339–349.
[10] Y. Oren, E. Korngold, N. Daltrophe, R. Messalem, Y. Volkman, L. Aronov, M. Weismann, N. Bouriakov, P. Glueckstern, J. Gilron, Pilot studies on high recovery BWRO-EDR for near zero liquid discharge approach, Desalination 261 (3) (2010) 321–330.
[11] R. Rautenbach, R. Habbe, Seeding technique for 'zero-discharge' processes, adaption to electrodialysis., Desalination. 84 (1-3).
[12] E. Korngold, L. Aronov, N. Daltrophe, Electrodialysis of brine solutions discharged from an RO plant, Desalination 242 (1-3) (2009) 215–227.
[13] E. R. Reahl, Reclaiming reverse osmosis blowdown with electrodialysis reversal, Desalination 78 (1) (1990) 77–89.
[14] S. Thampy, G. R. Desale, V. K. Shahi, B. S. Makwana, P. K. Ghosh, Development of hybrid electrodialysis-reverse osmosis domestic desalination unit for high recovery of product water, Desalination 282 (SI) (2011) 104–108.
[15] Y. Zhang, K. Ghyselbrecht, B. Meesschaert, L. Pinoy, B. Van der Bruggen, Electrodialysis on ro concentrate to improve water recovery in wastewater reclamation, Journal of Membrane Science 378 (1) (2011) 101–110.
[16] Y. Zhang, K. Ghyselbrecht, R. Vanherpe, B. Meesschaert, L. Pinoy, B. Van der Bruggen, Ro concentrate minimization by electrodialysis: Techno-economic analysis and environmental concerns, Journal of Environmental Management 107 (2012) 28–36.
[17] M. Fidaleo, M. Moresi, Electrodialytic desalting of model concentrated nacl brines as such or enriched with a non-electrolyte osmotic component, Journal of Membrane Science 367 (1) (2011) 220–232.
[18] R. K. McGovern, S. M. Zubair and J. H. Lienhard V, The cost effectiveness of electrodialysis for diverse salinity applications. Desalination 348, 2014, 57-65.
[19] H.-J. Lee, F. Sarfert, H. Strathmann, S.-H. Moon, Designing of an electrodialysis desalination plant, Desalination 142 (3) (2002) 267–286.
[20] S. A. Klein, Engineering Equation Solver, Academic Professional V9.438-3D (2013).
[21] Hydranautics, Membrane element ESPA2 max (2013) [cited 2014.01.20].
URL `http://www.membranes.com/docs/8inch/ESPA2%20MAX.pdf`
[22] General Electric Company, GE 2020 EDR Systems (2013).
[23] A. J. Giuffrida, Electrodialysis process for silica removal (1981).
[24] M. Fidaleo, M. Moresi, Optimal strategy to model the electrodialytic recovery of a strong electrolyte, Journal of Membrane Science 260 (1) (2005) 90–111.
[25] R. Robinson, R. Stokes, Electrolyte Solutions, 2002, Courier Dover Publications, Mineola, NY.
[26] O. Kuroda, S. Takahashi, M. Nomura, Characteristics of flow and mass transfer rate in an electrodialyzer compartment including spacer, Desalination 46 (1) (1983) 225–232.
[27] Electrical Research Association,1967 Steam Tables, Thermodynamic Properties of Water and Steam; Viscosity of Water and Steam, Thermal Conductivity of Water and Steam, 1967, Edward Arnold Publishers, London.
[28] T. Shedlovsky, The electrolytic conductivity of some uni-univalent electrolytes in water at 25 c, Journal of the American Chemical Society 54 (4) (1932) 1411–1428.
[29] J. Chambers, J. M. Stokes, R. Stokes, Conductances of concentrated aqueous sodium and potassium chloride solutions at 25 c, The Journal of Physical Chemistry 60 (7) (1956) 985–986.
[30] P. Tsiakis, L. G. Papageorgiou, Optimal design of an electrodialysis brackish water desalination plant, Desalination 173 (2) (2005) 173–186.
[31] A. Sonin, R. Probstein, A hydrodynamic theory of desalination by electrodialysis, Desalination 5 (3) (1968) 293–329.
[32] San Diego County Water Authority, Carlsbad desalination project (2012).
[33] U.S. Energy Information Administration, Annual energy outlook 2013, Tech. rep. (2013).

Nomenclature

Acronyms

ED	electrodialysis
ppm	parts per million, mg solute per kg solution
RO	reverse osmosis

Roman Symbols

A	area, m^2
C	cost/concentration, $/$m^3$/ mol/$m^3$
D	diffusion coefficient, m^2/s
E	potential, V
F	Faraday's constant, C/mol
h	channel height, m

i	current density, A/m^2
J	molar flux, mol/m^2·s
K_E	specific cost of electricity, \$/kWh
K_Q	cell-pair area normalised cost of equipment, \$/m^2
L_w	permeability to water, mol/m^2·s·bar
MC	marginal Cost, \$/m^3-ppm
$\dot{m}$	mass flow rate, kg/s
r	rate of return on capital, -
Re	Reynolds number, -
$\bar{r}$	area resistance, Ωm^2
p	power density, -
CR	cost ratio, -
S	salinity, kg salt/kg solution
Sc	Schmidt number, -
Sh	Sherwood number, -
t	solution transport number, -
T_s	membrane salt transport number, -
T_w	membrane water transport number, -
$\bar{T}$	integral ion transport number, -
V	flow velocity, m/s
V_{cp}	cell pair voltage, V
$\dot{V}$	volume flow rate, m^3/s
w	water
x	mole fraction, -
X	input parameter, various

Greek Symbols

Δ	difference
Λ	molar conductivity, Sm^2/mol
μ	chemical potential, J/mol
ν	viscosity, -
π	osmotic pressure, bar
ρ	density, kg/m^3
Σ	sensitivity, -
τ	time, years

Subscripts

am	anion exchange membrane
BP	bypass
c	concentrate
cm	cation exchange membrane
cu	counter ion
d	diluate
ED	electrodialysis
F	feed
m	at membrane surface
i	counting index
I	associated with current
$pump$	pump
P	product
RO	reverse osmosis
s	salt
w	water

Superscripts

hybrid	hybrid
solo	stand–alone
*	optimal
50%	operating at 50% recovery

Appendix A. Estimation of the growth of world brackish water desalination

Annualised growth in brackish desalination over the past ten years was calculated by considering the online capacity in the years 2003 and 2013. Data for new capacity brought online in each of the years 1993 until 2013 was obtained by summing together the new capacity online of 'River or low concentrated saline water (TDS 500 ppm - 3,000 ppm)' and 'Brackish water or inland water (TDS 3,000 - 20,000 ppm)' of plants tracked by Desaldata [1]. Online capacity in 2003 was then computed by summing together new capacity brought online in the years from 1993 to 2003, while online capacity in 2013 was computed by summing together new capacity brought online in the years 1993 to 2013.

Appendix B. Electrodialysis model details

Appendix B.1. Electrodialysis transport model

The total area of the electrodialysis system is broken into a series of cell-pair stacks. The diluate stream flows through these stacks in series. The concentrate streams are recirculated within each stack. To keep constant the volume of concentrate within each stack, a portion is bled off. The concentrate concentration in each stack is determined by the relative salt and water flux from diluate to concentrate:

$$x_c = \frac{J_s}{J_s + J_w} \tag{B.1}$$

where x_c is the mole fraction of salt in the concentrate, J_s is the net salt molar flux and J_w the net water molar flux from diluate to concentrate in a cell pair. The combination of the bleed streams from all stacks allows the computation of the outlet concentrate salinity from the ED system and the recovery ratio.

Salt, water and charge transport are modelled based upon the approach taken in previous work [18, 24]. Salt transport is modelled by a combination of migration and diffusion:

$$J_s = \frac{T_s^{cp} i}{F} - L_s \left(C_{s,c,m} - C_{s,d,m}\right) \tag{B.2}$$

and water transport by a combination of migration (electro-osmosis) and osmosis:

$$J_w = \frac{T_w^{cp} i}{F} + L_w \left(\pi_{c,m} - \pi_{d,m}\right) \tag{B.3}$$

T_s^{cp} and T_w^{cp} are the overall salt and water transport numbers for the cell pair, L_s and L_w are the overall salt and water permeabilities of the cell pair and all four quantites are considered independent of diluate and concentrate salinity. C denotes concentration in moles per unit volume and π osmotic pressure (calculated employing osmotic coefficients for aqueous NaCl from Robinson and Stokes [25]). F is Faraday's constant and the subscripts s, c, d and m denote salt, the concentrate stream, the diluate stream and the membrane-solution interface. The difference between bulk and membrane wall concentrations and osmotic pressures is accounted for by a convection-diffusion model of concentration polarisation:

$$\Delta C = -\frac{\left(\bar{T}_{cu} - t_{cu}\right)}{D}\frac{i}{F}\frac{2h}{\mathrm{Sh}} \tag{B.4}$$

where D is the solute diffusivity (distance squared per unit time), h is the channel height and t_{cu} is the counter-ion transport number in the diluate and concentrate solutions and is approximated as 0.5 for both anions and cations. $\bar{T}_{cu}$ is the integral counter-ion transport number in the membrane that accounts for both migration and diffusion. $\bar{T}_{cu}$ is the integral counter-ion transport number in the membrane that accounts for both migration and diffusion.

$$\bar{T}_{cu} \approx \frac{T_s^{cp} + 1}{2}. \tag{B.5}$$

This expression would be exact were diffusion within the membrane to be negligible and the counter-ion transport number to be equal in anion and cation exchange membranes. Sh, the Sherwood number is computed using the correlation obtained by Kuroda et al. [26] for spacer A in their analysis:

$$\mathrm{Sh} = 0.5\mathrm{Re}^{1/2} Sc^{1/3} \tag{B.6}$$

where Sc is the Schmidt number, calculated using the limiting diffusivity of NaCl in water [25] and the kinematic viscosity of pure water ν [27], both at 25°C. Re is the Reynolds number defined as:

$$\mathrm{Re} = \frac{2hV}{\nu} \tag{B.7}$$

where V is the mass averaged velocity in the channel.

The cell pair voltage, is represented as the sum of ohmic terms and membrane potentials:

$$V^{cp} = i\left(\bar{r}_{am} + \bar{r}_{cm} + \frac{h_d}{\sigma\Lambda_d C_d} + \frac{h_c}{\sigma\Lambda_c C_c}\right) + E_{am} + E_{cm} \tag{B.8}$$

where Λ is the molar conductivity, itself a function of concentration [28, 29], h denotes channel height and σ denotes the spacer shadow factor. Membrane surface resistances, denoted $\bar{r}$, are considered to be independent of salinity. Junction potentials associated with concentration polarisation are neglected, while the sum of the anion and cation membrane potentials $E_{am} + E_{cm}$ is computed considering quasi-equilibrium migration of salt and water across the membranes (based on the approach of Prentice [**?**]):

$$E_{am}+E_{cm} = T_s^{cp}\frac{1}{F}(\mu_{s,c,m} - \mu_{s,d,m}) + T_w^{cp}\frac{1}{F}(\mu_{w,c,m} - \mu_{w,d,m}) \tag{B.9}$$

where μ_s denotes the chemical potential of salt and μ_w the chemical potential of water; both calculated employing osmotic coefficients and NaCl activity coefficient data from Robinson and Stokes [25].

Knowing the inlet and outlet salinities from each stack, the salt flux, water flux and cell pair voltage allows the computation of energy, area and concentrate salinity for each stack.

Appendix B.2. Evaluation of the stack voltage

The cell pair voltage is set such that the ratio of the current density to the theoretical limiting current density is approximately equal to 70% throughout the stack. This is done by considering a reference point in the system where the salinity is 350 ppm. The limiting current density at this point is calculated using:

$$i_{lim} = -\frac{D}{\bar{T}_{cu} - t_{cu}}\frac{\mathrm{Sh}}{2h}FC_d. \tag{B.10}$$

Given this limiting current density the cell pair voltage V_{cp}^{350ppm} is solved for by setting $i = 0.7 i_{lim}$ within Eq (B.8). This cell pair voltage is then employed across the entire system. Employing the same cell pair voltage across the entire system approximately maintains the same ratio of i/i_{lim} throughout. This is because both the current density and the limiting current density both scale approximately with the diluate concentration. At higher diluate concentrations than considered in this paper this approximation breaks down as the cell pair resistance no longer scales with the diluate resistance when membrane resistances become important.

Appendix B.3. Electrodialysis cost model

The stand–alone electrodialysis system and the electrodialysis subsystem are costed on the basis of system size, represented by membrane area, and energy consumption. Equipment costs are assumed to scale with membrane area and are costed employing an equipment cost per unit cell pair area K_Q [19, 30]. The equipment costs are amortised considering a plant life τ and an annualised cost of capital of r:

$$C_Q = \frac{1}{\dot{V}_{d,o}}\frac{K_Q \sum_i A_i}{\frac{1}{r}\left[1 - \left(\frac{1}{1+r}\right)^{\tau}\right]} \tag{B.11}$$

where A_i is the area of a single-stage and $\dot{V}_{d,o}$ is the volume flow-rate of diluate out of the final ED stage. Energy costs are computed by taking the product of stack power consumption and the cost of electricity K_E:

$$C_E = \frac{K_E}{\dot{V}_{d,o}} \sum_i V_{cp} i_i A_i \tag{B.12}$$

where i_i is the current density in stage i. Energy required for pumping power is neglected as it may be shown to be negligible relative to energy required to drive desalination (Appendix G). The combination of equipment and energy costs:

$$C = C_Q + C_E \tag{B.13}$$

gives the specific cost of water C. A summary of the membrane (validated experimentally by Fidaleo and Moresi [17]), cell-pair geometry and financial parameters employed are provided in Table B.2.

Appendix C. Estimation of specific equipment costs

Sajtar and Bagley [**?**] reviewed the capital costs of electrodialysis plants removing between 0 and 2,000 mg/L of total dissolved solids from a feed stream. They found capital costs to scale approximately linearly with product flow rate such that the capital cost per unit of production rate was \$568/(m^3/day).

Running the model of Appendix B, with a feed salinity of 2,350 ppm, a product salinity of 350 ppm (*e.g.* approximately 2,000 mg/L of TDS removal), and the voltage set such that the current density is 70% of its limiting value in the final stage (0.8 V per cell pair), yields an area requirement of 0.39 m^2 of cell pair area/(m^3/day). The combination of this information on capital cost from Sajtar and Bagley [**?**] with the area requirements predicted by the model results in estimated specific equipment costs of approximately \$1500/m^2 cell pair area.

Appendix D. Validation of energy consumption

Sajtar and Bagley [**?**] reviewed the energy consumption of electrodialysis plants removing between 0 and 2,000 mg/L of total dissolved solids from a feed stream. Though there is a positive correlation between salt removal and electrical consumption there is significant scatter in the data at these levels of TDS removal, with energy consumption varying between 0.1 and 1 kWh/m^3. The ED model, run with the conditions described in Appendix C, predicts energy consumption of 0.79 kWh/m^3, which falls between these limits. Of course, energy consumption will depend upon stack design parameters such as diluate channel height, the spacer shadow factor and the voltage applied per cell pair.

Symbol	Value	Ref.
Membrane Performance Parameters		
T_s	0.97	[17]
T_w	10	[17]
L_w	1.4×10^{-4} mol/bar-m^2-s	[17]
L_s	1.4×10^{-8} m/s	[17]
$\bar{r}_{am}, \bar{r}_{cm}$	2.8 Ω cm^2	[17]
Solution Properties		
D	1.61×10^{-9} m^2/s	[25]
t_{cu}	0.5	[31]
ν	8.9×10^{-7} m^2/s	[27]
ρ	9.97×10^{2} kg/m^3	[27]
Flow Properties/Geometry		
h	0.4 mm	[17, 19][a]
V	0.05 m/s	[19][b]
σ	0.7	[24]
N	20	-
Re	44.8	calc.
Sh	27.5	calc.
Cost Parameters		
K_Q	1,500 \$/m^2 cell pair	Appendix C
τ	20 years	-[c]
r	10%	[33][d]
K_E	0.065 \$/kWh	[34][e]
Operational Conditions		
S_F	3,000 ppm	-
V^{cp}	0.8 V	[19]

[a] Lee et al. [19] suggest 0.65 mm, while Fidaleo et al. [17] employ 0.7 mm;
[b] Lee et al. [19] suggest 0.075 m/s
[c] increased from Lee et al. [19] and Tsiakis et al.'s [30] suggestion of a 6 year plant life
[d] Returns on an entire project are assumed to be twice the 4.78% rate paid on bonds issued to finance the Carlsbad desalination plant [33].
[e] based on conventional combined cycle natural gas plants coming online in 2018 at 0.067 \$/kWh

Table B.2: Electrodialysis Model Parameters

Appendix E. Hybrid model details

Similar equations apply for the computation of masses and salinities within the simple and recirculated hybrid systems (Fig. E.9). The conservation of total mass and salt mass at the points of product blending,

$$\dot{m}_{RO,P} + \dot{m}_{ED,P} = \dot{m}_P \tag{E.1}$$

$$S_{RO,P}\dot{m}_{RO,P} + S_{ED,P}\dot{m}_{ED,P} = S_P\dot{m}_P, \tag{E.2}$$

and on the RO units,

$$\dot{m}_{RO,P} + \dot{m}_{ED,F} = \dot{m}_{RO,F} \tag{E.3}$$

$$S_{RO,P}\dot{m}_{RO,P} + S_{ED,F}\dot{m}_{ED,F} = S_{RO,F}\dot{m}_{RO,F}, \tag{E.4}$$

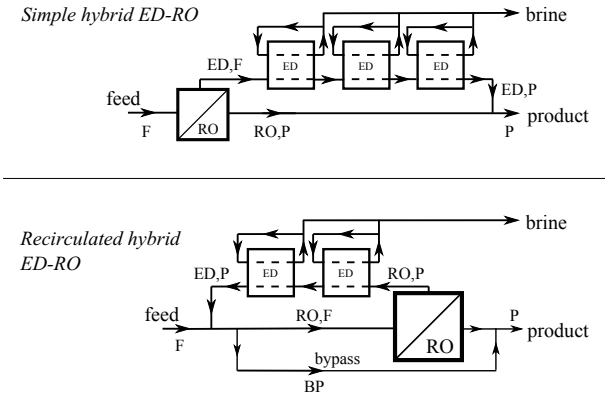

Figure E.9: Simple and recirculated hybrid systems with streams labelled

are the same for both hybrids, as is the consideration of the recovery ratio of the RO system,

$$\dot{m}_{RO,P}(1 - S_{RO,P}) = 50\% \times \dot{m}_{RO,F}(1 - S_{RO,F}). \quad \text{(E.5)}$$

The main difference arising is that the determination of masses and salinities is fully specified by the above equations in the case of the recirculated hybrid system whereas the simple hybrid system requires the above equations to be simultaneously solved with the set of coupled non-linear equations describing the ED system, which may be written as:

$$\dot{m}_{ED,P} = \text{fn}(\dot{m}_{ED,F}, S_{ED,F}, S_{ED,P}). \quad \text{(E.6)}$$

For both hybrid systems and the stand–alone ED system the specific cost of water (based on the ED diluate outlet flow rate) is available from the ED model and may be written:

$$C_{ED} = \text{fn}(\dot{m}_{ED,F}, S_{ED,F}, S_{ED,P}) \quad \text{(E.7)}$$

The overall cost of the standalone ED system and the hybrid ED-RO system are then equated:

$$C_{ED}^{solo} \frac{\dot{m}_P}{\rho_P} = C_{ED}^{hybrid} \frac{\dot{m}_{ED,P}}{\rho_{ED,P}} + C_{RO} \frac{\dot{m}_{RO,P}}{\rho_{RO,P}} \quad \text{(E.8)}$$

and divided across by C_{ED}^{solo} to yield:

$$\frac{\dot{m}_P}{\rho_P} = \frac{C_{ED}^{hybrid} \dot{m}_{ED,P}}{C_{ED}^{solo} \rho_{ED,P}} + CR^* \frac{\dot{m}_{RO,P}}{\rho_{RO,P}} \quad \text{(E.9)}$$

where CR^* is the quantity of interest, the critical cost ratio of water from the single-stage RO system to the stand–alone ED system.

Appendix F. Analysis of the recovery ratio from stand–alone, simple hybrid and recirculated hybrid systems

The recovery ratio, *RR*, defined as the ratio of the mass flow rate of water in the product stream from a system to the mass flow rate of water in the feed stream to a system, is plotted as a function of system product salinity in Fig. F.10, employing operating conditions identical to those in Fig. **??**. There is little difference between the recovery ratios achieved with the three systems. Increases in the desired product water salinity cause the recovery ratio to increase, but only to a small extent. Recovery ratios are high because, in all three systems, water is only lost from the feed stream due to electro-osmosis or osmosis. Water loss via electro-osmosis is almost identical in all three systems since the volume of water transported by electro-osmosis depends upon the rate of salt removal from the feed, and the rate of salt removal is almost identical in all three systems since they are compared considering the same feed and product salinities. The level of water transport by osmosis in each system is dictated by the concentration difference between the diluate and concentrate streams, which drives diffusion, and also the total membrane area over which osmosis can occur. The ED unit within the recirculated hybrid is most compact as it operates at the highest diluate salinities (higher current densities) and thus exhibits the lowest level of osmosis and the highest recovery ratio. Conversely, the stand–alone ED system is the least compact, as the range of diluate salinities over which it removes salt is the lowest (low current densities), and thus osmosis is higher and recovery lower. In all three cases, recovery ratios increase with product salinity as the ED units become more compact, thus reducing water losses via osmosis. These recovery ratios provide an approximate upper bound on what is achievable in a real system. In practise, recovery ratios may be reduced by blending a portion of the feed stream to each electrodialysis unit with the concentrate stream in order to slow the precipitation of supersaturated salts in the concentrate.

Appendix G. Assessment of electrodialysis power requirements for pumping

The power consumption associated with drawing a current and pumping fluid through the channels may be compared on the basis of unit cell pair area. Power consumption associated with salt removal,

$$p_I = V_{cp} i, \quad \text{(G.1)}$$

where V_{cp} is the cell pair voltage and i is the current density, is minimum in the final ED stack where the diluate salinity is lowest (350 ppm), the resistance

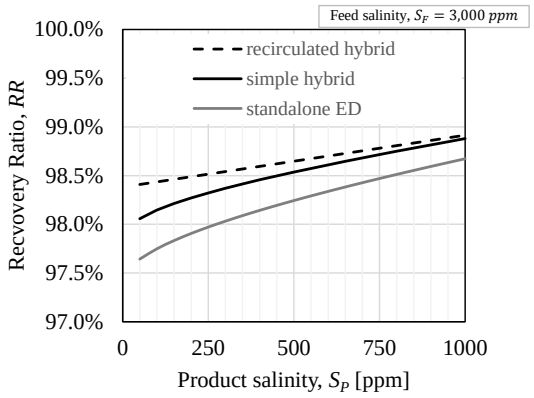

Figure F.10: System recovery ratios

highest and thus, for a constant cell pair voltage, the current density lowest. Power consumption associated with pumping may be quantified by considering viscous dissipation per unit cell pair area:

$$p_{pump} = 2Vh\frac{\Delta P}{L} \tag{G.2}$$

where the factor of 2 accounts for viscous dissipation in the diluate and concentrate channels, the product Vh is the volumetric flow rate per unit channel width through a cell pair and $\frac{\Delta P}{L}$ is the pressure drop per unit length, which may be found via the friction factor, defined as:

$$f = \frac{\Delta P}{0.5\rho V^3 \frac{L}{2h}} \tag{G.3}$$

where ρ, the fluid density, is approximated by the density of pure water [27]. A friction factor correlation, such as that obtained by Kuroda et al. [26] for spacer A in their analysis,

$$f = 9.6Re^{-1/2}, \tag{G.4}$$

allows the computation of p_{pump}. Given the parameters of Table B.2, the power associated with drawing current at 350 ppm TDS is over 620 times that associated with viscous dissipation.